Evaluation of different micromixers by CFD simulations for the anionic polymerisation of styrene

Dirk Ziegenbalg¹, Christoph Kompter¹, Friedhelm Schönfeld² and Dana Kralisch^{1,*}

¹ Institute for Technical Chemistry and Environmental Chemistry, Friedrich-Schiller University, Lessingstr. 12, D-07749 Jena, Germany, e-mail: dana.kralisch@uni-jena.de ² Hochschule RheinMain, Am Brückweg 26, D-65428 Rüsselsheim, Germany

Abstract

To ensure a sufficient reaction control, including fast mixing and heat removal, microstructured devices were chosen to conduct anionic polymerisations. To decrease the experimental effort and the resulting costs, a numerical approach was followed to apply decision support during experimental planning. Semi-quantitative CFD calculations were used to determine the best suited micromixer out of a collection of different devices. Using the numerical investigated micromixers for experimental investigations, the general order gained from CFD calculations was confirmed. It could be shown that CFD calculations can beneficially be used to rank micromixing devices for specific process conditions and synthesis tasks.

Keywords: anionic polymerisation; micromixer; reaction control; simulation.

List of abbreviations

area (m²)

Init

initiator

/s)
g quality

maximum max perf perfect Mono monomer rel relative segregated seg sum/summed sum **Greek symbols** viscosty (Pa×s) density (kg/m³) $\Delta_{p}H$ reaction enthalpy (kJ/mol)

1. Introduction

Modern chemical process design has to be fast, flexible and low material consuming. Thus, tools and devices for screening prior to more detailed investigations, e.g., by using parallel reactors or flow chemistry in microreactors gain an increasing role in chemical laboratories. In this context, also new questions, such as for the best suited reaction devices, mixing structures or operation parameters arise. Several of these questions can be answered by using the capabilities of modern computer technology, e.g., by computational fluid dynamics (CFD) accompanying experimental planning. The CFD-assisted approach is especially helpful in the case of demanding reactions that require a sophisticated handling and control. In this context, CFD can become a valuable and powerful tool to support a fast and knowledge-based process design. Utilising numerical tools can provide decision support for the choice of best suited reactor devices, e.g., through an enhanced understanding of mixing phenomena under specific process conditions. Additionally, it is possible to screen the influence of process parameter variations on the resulting mixing efficiency.

In the present study, we show how CFD studies can support the understanding of micro kinetic and mass transport phenomena of a highly exothermic, experimentally challenging synthesis. The anionic polymerisation of styrene as a part of rod-coil-copolymer preparation is commonly performed in a batch process and is affected by a number of disadvantages, such as low heat transfer capabilities or low mixing performance. The results show that transferring a batch process to an intensified continuously running microreaction process can be supported by CFD prior to experimental investigations.

1.1. The model synthesis

The work presented here is an essential part of ongoing research activities to intensify the syntheses of block copolymer with optoelectronic properties.

^{*} Corresponding author

The block copolymers are built-up from flexible non-conjugated coils (polymer backbone, e.g., polystyrene, polymethyl methacrylate, butadiene) and rigid conjugated rods (chromophore) to gain self-assembling properties, generating ordered supramolecular structures. To precisely control the optoelectronic properties of the final polymer, a very narrow molecular weight distribution and a polydispersity index (PDI) of <1.2 are indispensable. Then, manipulating of the optoelectronic properties of the polymer, going beyond the possibilities of a single chromophoric rod, shall be realisable by, e.g., adjusting the chain length. The final goal is the fast screening and optimisation of rod-coil-copolymers which can be used, e.g., as p-conducting substances for organic solar cells.

The flexible coils are commonly synthesised by anionic polymerisation to gain a narrow molecular weight distribution. The reaction kinetics are very fast and during the reaction a vast amount of heat is released [1, 2]. The anionic polymerisation of styrene shows a reaction enthalpy of $\Delta_R H$ =-72, 84 kJ/mol (17,400 cal/mol) at 400 K [3]. The rate constant for the propagation is kp=500 l/mol/s [4]. Conventionally, anionic polymerisations are conducted in full glass apparatuses under a complete inert atmosphere, because oxygen and protic molecules terminate the chain reaction [5]. To get rid of the heat release problem, the reaction temperature for the anionic polymerisation is usually -78°C.

As initiator usually organometallic substances such as butyllithium are applied. Anionic polymerisation facilitates the synthesis of polymers with a very narrow molecular weight distribution, if initially a homogeneous distribution of initiator and monomer is ensured by very fast mixing. This guarantees a synchronous start of all polymerisation chains and with this a homogeneous product quality. The uniformity of polymers is usually expressed by the PDI representing the ratio of weight average molecular weight and number average molecular weight.

1.2. Polymerisation in microreactors

Microreaction technology is a modern tool to achieve high reaction control [6–11]. The main idea of this concept is to reduce the overall dimensions of components which are in contact with the reacting fluids. In detail, the dimensions of the devices range from several ten micrometers to approximately 2000 μ m. With this, the diffusion lengths are drastically reduced leading to faster equilibrating of diffusion-like processes (mass diffusion, heat conduction). The small dimensions and their consequences sum up to some significant advantages compared to conventional batch vessels, e.g., very fast heat and mass transfer, small hold-up and inherent safety.

The use of microreactors enhances reaction control and enables the conduction of very fast reactions with strong heat release such as fluorinations, chlorinations or ozonisations [12–17].

Additionally, in the case of inert operation, continuous processing in microreactors can be beneficial, because it is only necessary to generate an inert atmosphere for the reactant vessels. All the following devices, pipes, etc., stay inert after a sufficient starting time. Before starting the polymerisation the experimental setup can be cleaned by simply rinsing with pure solvent. Additionally, it is easier to change operation conditions such as initiator/monomer ratio, temperature, residence/reaction time, etc.

Several groups showed that polymerisation reactions can be beneficially conducted within microreactors, as the enhanced heat and mass transfer capabilities result in an improved reaction control and enable narrow molecular weight distributions [18–20]. A first report by Bayer et al. showed that the high mixing capabilities of micromixers can be utilised to prevent static mixers from clogging [21]. Later on, atom-transfer-radical-polymerisations were realised within microreactors [22, 23]. The successful realisation of a carbocationic polymerisation was demonstrated by Nagaki et al. [24]. In subsequent work the authors extended the approach to additional monomers [25, 26]. Free radical polymerisations in microsystems were also accomplished and patented [27, 28].

Numerical studies from the group around Serra supported the experimental findings for free radical polymerisation [29–31]. The group further investigated the nitroxide-mediated block copolymerisation of n-butyl acrylate and styrene and could show that the PDI can be predicted by a form factor of the micromixer [32, 33].

Anionic polymerisations in microreactors were first implemented by Honda et al. [34]. It could be shown that intensifying the mixing process significantly reduces the PDI. In further work, the authors conducted the polymerisation with high reaction control for 2 months [35]. Anionic polymerisations were revisited by the groups of Yoshida [36, 37] and Frey [38] to demonstrate the synthesis of block copolymers. The influences of mass transfer on reaction control under these conditions were shown by Iida et al. [39].

Based on these studies, we expected the following advantages from the use of microreactors instead of full glass batch apparatuses for our purposes:

- improved process control and constant high product quality of rod-coil-copolymers from continuous operation,
- significant decrease of time for experimental investigations due to the possibility of fast screening of different process parameters and chromophores in one experimental run,
- simplified transfer of results from experimental to production scale through, e.g., numbering-up or smart dimensioning.

However, it also became clear that one challenge from the reaction engineering point of view was to realise a reaction plant offering a sufficient mixing speed in combination with fast heat removal. Thus, the focus of the presented study lies on the evaluation of different micromixers which can be used for achieving the necessary reaction control for the anionic polymerisation of the flexible part of the semiconducting polymer with a PDI<1.1 (flexible coil) in front of a blocking with the chromophore (overall PDI<1.2). To decide for the best suited mixing structure from the wide range of available micromixers, we used CFD calculations on a semi-quantitative level.

2. Equipment evaluation by CFD calculations

An important task during the development of a reaction plant is to choose appropriate equipment including pumps, pipes, mixers, reactors, etc. Usually such investigations are done in a more or less empirical way. This means that all devices have to be investigated experimentally, as long as no adequate knowledge for the target reaction system is available. Consequently, the investigations often become time-consuming and expensive. Costs mainly arise from investment expenditures for the devices and experimental costs including expenses for working staff and consumables. This is aggravated by the fact that usually a high number of potential devices is available.

As a consequence of the ongoing developments in computer technology, a broad range of numerical tools have been developed, allowing to solve strongly coupled (differential) equations. This is, e.g., necessary to solve fluid dynamic problems. One advantage of such a numerical approach is the possibility to obtain a deep insight into the fundamental fluid dynamics within the investigated device. Furthermore, it is possible to decrease development time through the reduction of experimental efforts.

Today, available computer performance is not only sufficient to obtain global and/or qualitative information of the investigated system but, instead, local and/or quantitative information become computable in feasible times. In the present context, we use CFD simulations to evaluate different micromixing devices which facilitate sufficiently fast mixing for the continuously operated anionic polymerisation.

As stated before, thorough and fast mixing is one of the vital points to run anionic polymerisations. For the CFD-based mixing evaluation we use the mixing residuum as an integral measure for the degree of mixing. In this regard, the performed CFD simulation is semi-quantitative. The mixing residuum allows to compare and classify different mixers for the relevant operation conditions for anionic polymerisations, whereas details of the actual reaction are not considered. The chosen approach keeps the computational effort manageable and helps to identify the best suited micromixers. Moreover, the CFD results can be contrasted to the experimental findings.

3. Micromixers

Currently, a large number of micromixers is available. They usually differ in channel size and mixing principle. Although numerous publications dealing with micromixers are available, there are only a few of them which are helpful for the selection of appropriate mixers for specific reaction. This is, on the one hand, due to the fact that in most cases individual micromixers are investigated and characterised. On the other hand, it is often difficult if not impossible to compare the results from different publications, because usually different experimental methods were used. Recently, Falk et al. condensed published results for different micromixers characterised by the Villermaux-Dushman protocol by harmonising the experimental data [40]. They showed that within

the investigated set of micromixers the achievable mixing time can be correlated to the specific energy dissipation. In a subsequent study, the same authors proposed a detailed standardised Villermaux-Dushman protocol for the experimental characterisation of micromixers [41].

However, the information in the mentioned studies can not readily be transferred to the present study targeting at a continuous reaction system for anionic polymerisation. One reason for this lies in the intention to use considerably asymmetric flow rates. In addition, this comes from the idea to reduce the ecological footprint of the process (for more detailed information see section 4.3). With a view on the dedicated process window for the anionic polymerisation, a micromixer is searched which enables a sufficient fast mixing over a wide range of operation conditions for simplified transfer to a future production plant. Under these premises it is also interesting to investigate micromixers not ranked in the study of Falk et al.

4. Mathematical framework

4.1. CFD calculations

As mentioned above, in the present context the investigations of different micromixers were done by means of CFD simulations. The numerical results presented in this work are based on the solution of the incompressible Navier-Stokes equation (neglecting gravitational effects)

$$\rho \frac{\partial \mathbf{v}}{\partial t} = \rho \ \nabla \ \eta \nabla^2 \ \nabla p \tag{1}$$

where v denotes the fluid velocity vector field, ρ its density and p is the pressure. For incompressible fluids the continuity equation reduces to:

$$\nabla v = 0.$$
 (2)

The boundary conditions were specified as follows: no-slip conditions were assumed at the channel walls. At the inlets the mass flow rate of each species was defined and a static relative pressure of p=0 Pa was defined at the outlet.

The mass transport is governed by the convection-diffusion equation:

$$\frac{\partial c}{\partial t} = -v \nabla_C + \nabla(D \nabla_C), \tag{3}$$

with c being the species concentration and D being the binary diffusion coefficient. The investigated micromixers were simulated under steady state.

It is possible to quantify the mixing progress by analysing the species distribution on specified cross-sections. This can be done by calculating a so-called mixing residuum [42]:

$$r = \frac{1}{4 \cdot A \cdot w_{i,perf} \cdot (1 - w_{i,perf})} \iint_{(s)} \left| w_i(x, y, t) - w_{i,perf} \right| dA, \tag{4}$$

where A denotes the area of the cross-section considered, $w_i(x; y; t)$ is the mass fraction of species i at position x, y and time

t and $w_{i,perf}$ being the mass fraction of species i in a perfectly homogeneous mixed solution. The mass fraction of species i is defined as:

$$w_{i} = \frac{\dot{m}_{i}}{\sum_{i=1}^{n} \dot{m}_{i}},\tag{5}$$

where $\dot{m_i}$ and $\dot{m_j}$ denote the mass flow rates of species i and j. The total number of all species is n. By definition, the mass fraction ranges from 0 to 1. This results in the fact that the mixing residuum r can reach values between 0 and 0.5. A value of 0.5 indicates a completely unmixed solution, whereas 0 indicates a homogeneous mixed solution.

Different micromixers naturally have different dimensions and with this different inner volumes. To compare the mixing performance of different micromixers it is necessary to specify a comparative value. Such a value is the time needed to achieve a specified value of the mixing residuum (indicating the mixing quality). In this work, a homogeneity of 95% was used as the target value meaning a mixing residuum of r=0.025. To ensure comparability between different micromixers, the mixing time t_{M.95%} was defined as follows:

$$t_{\text{M},95\%} = t_{\text{R}} \times S_{95\%}.$$
 (6)

The space time of the mixer is represented by $t_{\rm R}$ and $s_{95\%}$ is the relative mixer length needed to reach the desired homogeneity. The space time can be calculated as follows:

$$t_R = \frac{V_R}{\dot{V}_{\Sigma}},\tag{7}$$

where $V_{\rm R}$ denotes the mixer volume and \dot{V}_{Σ} denotes the total volumetric flow rate. Despite the volumetric relationship of the space time the relative mixer length was chosen for the calculations. In case of using a relative volume, dead volumes/zones have to be excluded when the value is determined. The definition of such areas would require subjective decisions and was therefore avoided.

The polymerisation and all other chemical reactions were not included in the CFD simulations. As the inherent reaction timescales are fast the polymerisation is predominantly mass transfer limited. To overcome or at least to minimise the mass transfer limitation the CFD study focuses on the pure mixing process.

Calculations were done on an Intel[®] Core[™] i7 quad-core CPU using 12 GB RAM. Software packages ANSYS CFX 12 and ANSYS ICEM CFD (ANSYS, Inc., Canonsburg, PA, USA) were used.

4.2. Micromixers

Five different micromixers have been investigated regarding their mixing performance in the case of the anionic polymerisation of styrene. For all mixers geometric models were realised representing the core mixing structure. Feed lines and periphery were neglected to simplify the models.

As a reference device a simple Y-mixer connected to a straight reaction channel was investigated. The round channels

had an inner diameter of $1000 \, \mu m$ (Figure 1). The model used for CFD calculations corresponds to a Y-mixer available from the Little Things Factory (LTF) GmbH, Ilmenau, Germany. The mixing principle of this mixer is based on pure diffusion between two fluid lamellae. This holds up to a certain flow rate when shear forces induce secondary fluid motion [43–47]. This mixer is subsequently referenced as the "Y-mixer" within the following discussion.

As a second mixer a modified Y-mixer was studied. In addition to the Y-mixing zone this mixer comprises a residence channel with chicanes as shown in Figure 2A. The chicanes are dedicated to induce circulations perpendicular to the (main) flow direction. Inducing circulations aims towards clinching and stretching of the fluid lamellae and with this increasing the interfacial area. This mixer model is similar to the LTF MSLT-mixer and had the same inner channel diameter as the Y-mixer.

As a third mixer from LTF the so-called LTF ST-mixer was investigated (Figure 2B). Owing to obstacles within the channel, the fluid is continuously redirected in a way that can be described as split-and-recombine (SAR) [48, 49]. The SAR principle increases the interfacial area through serially multiplying the number of fluid lamellar. Depending on the number n of SAR steps, the number of lamellar is 2^{n+1} and consequently the (diffusive) mixing time is reduced by a factor of 4^n . The overall channel width of this mixer is $1200 \,\mu\text{m}$ including all obstacles. The obstacles reduce the actual channel width at several positions down to approximately $250 \,\mu\text{m}$.

The caterpillar micromixer from the Institut für Mikrotechnik Mainz (IMM) also relies on the SAR principle [49–51]. Compared to the ST-mixer the geometry of the caterpillar mixer is simpler (compare Figure 2B and C). It consists of 12 or 8 elements. Within each element the fluid undergoes one SAR step. This results in 2048 or 128 lamellar, respectively, in the ideal case. The caterpillar micromixer is available with different channel widths of 300 μm , 600 μm or 1200 μm . As the absolute lamellar thickness has a distinct effect on the mixing time, we have taken into account all previously mentioned channel widths. The lengths of the mixing elements were proportional adapted to the variations of the channel width. The 300 and 600 μm versions consisted of 12, whereas the 1200 μm version consisted of 8 elements. The

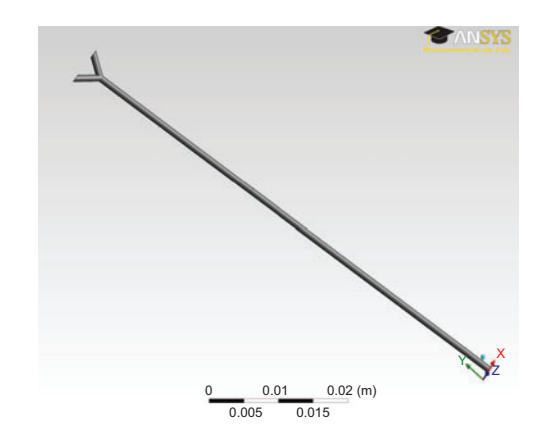


Figure 1 Model domain of the Y-mixer used in the CFD studies.

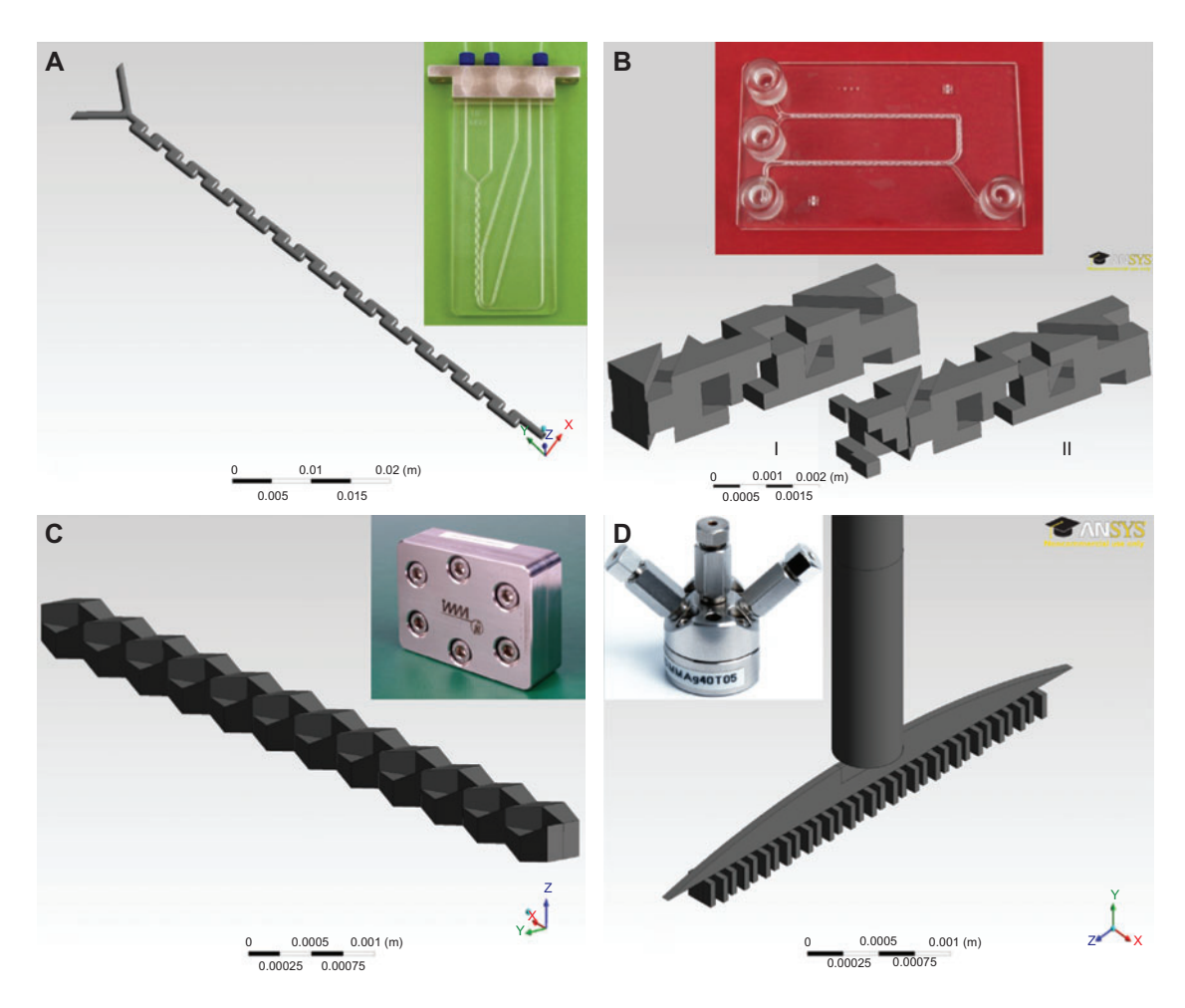


Figure 2 Investigated micromixer. (A) Chicane mixer, (B) ST-mixer, (C) caterpillar mixer, (D) interdigital mixer. The large figures show the model domain used in the CFD studies. The insets show the real micromixer.

mixer will be referenced as "caterpillar mixer" supplemented by the corresponding channel width.

Finally, an interdigital mixer from IMM was considered. This mixer uses the parallel multilamination principle [52]. This means that the (e.g., two) main fluid streams are subdivided into several substreams, which are reunified in such a manner that the substreams of the different fluids are shifted against each other to increase the total number of lamellae. The mixer had 16 inlet channels for each fluid with a width of 45 μ m. They are then united into a circular outlet channel of 500 μ m diameter (Figure 2D). The mixing speed of this mixer is further enhanced by geometric focusing after the reunification zone. This results in an additional reduction of the fluid lamellar width and an acceleration of the mixing process [53].

4.3. Process conditions

To ensure comparability to the experimental work started in parallel, the substance system was adopted from the process parameters to be investigated in the context of the anionic polymerisation of styrene. Concentrations and physical substance properties were defined with realistic values and are summed up in Table 1. A diffusion coefficient of $D=10^{-9}$ m²/s was assumed, which is a typical value for liquid systems [57]. As every additional component within the component system increases the equation system for the simulation, the actual initiator was neglected, instead solvent plus initiator is considered as a single species, the physical properties which were assumed to be equal to those of the pure solvent used to stabilise the initiator. This is possible because the concentration of the initiator used in the experimental work was relatively low ($c_{tnit} \le 0$, 1 mol/l).

Two fluids were defined at the inlet. First, a so-called monomer solution consisting of 50 mass percent tetrahydro-furane (THF) as solvent and 50 m% of the monomer styrene

Table 1 Physical properties of the used substances.

	M/(g/mol)	$\rho/(kg/m^3)$	$\eta/(Pa\times s)$
n-Hexane	86.18	655.2	0.298×10 ⁻³
Styrene	104.15	902	0.695×10^{-3}
Tetrahydrofurane	72.11	889	0.4631×10 ⁻³

Values for hexane were taken from [54]. The physical properties of styrene can be found in [55]. The properties of tetrahydrofurane were taken from [56].

was defined. The second fluid, the so-called initiator fluid, consisted of pure n-hexane.

One focus of the overall work was to reduce the ecological footprint of the developed process [58]. This should be achieved by taking possible future ecological impacts into account, already during the development phase. The simplified Life Cycle Assessment, performed in parallel to the ongoing computational and experimental work, led to the insight that a reduction of the amount of solvents has the highest optimisation potential of all process parameter variations investigated. Within the numerical and experimental studies this was reflected by, e.g., a variation of the initiator flow rate, whereas the monomer flow rate was kept constant as well as the concentration of the monomer in the solution. To realise a constant amount of initiator per time, an adaptation of the initiator concentration was necessary for experimental studies. The investigated process conditions are summarised in Table 2. The experiments conducted in parallel typically aimed at a theoretical number-average molecular weight of 3000 g/mol.

5. Results

5.1. Mesh dependencies

For the Y-mixer and the chicane mixer meshes with approximately 16.4 million or 18 million tetrahedral elements were used, respectively. The models of the caterpillar mixers consisted of approximately 3.3 million structured hexahedral elements. For all models of the caterpillar mixer a corresponding scaled mesh was used. The only differences between the meshes were the dimensions. The mesh of the interdigital mixer was assembled primarily from hexahedral elements. It was possible to use approximately 4.1 million elements.

For the ST-mixer a different approach was used to ensure sufficient resolution. The geometry was split into two parts. The first part included the entry/contacting zone for the two fluids (Figure 2B, I), whereas the second part is the repeating unit of the mixer (Figure 2B, II). Both parts consisted of approximately 16.7 million tetrahedral elements. Calculations were carried out in such a way that the first part was calculated and subsequently the second part was computed using the results from the outlet of the first part as inlet conditions for the second part.

In a next step, the influence of discretisation errors was analysed. Therefore, mesh dependency studies were carried out. The approach used for all different micromixers was as follows. In each case we started with the mesh having the

Table 2 Investigated process conditions.

Initiator		Monomer		Ratio
$\dot{m}_{\rm Init}/({\rm g/s})$	$\dot{V}_{\rm Init}/({ m ml/min})$	$\dot{m}_{\mathrm{Mono}}/(\mathrm{g/s})$	$\dot{V}_{\mathrm{Mono}}/(\mathrm{ml/min})$	init/mono
0.03	2.74809	0.03	1.99	1:1
0.00906	0.82992	0.03	1.99	1:3.3
0.00226	0.20702	0.03	1.99	1:13.3
0.000566	0.05185	0.03	1.99	1:53
0.000283	0.02592	0.03	1.99	1:106

maximum number of elements, which was manageable. This is termed 100% mesh in the following. Subsequently, the element number of the 100% mesh was reduced down to 75%, 50%, 40% and 25%. After solving the velocity filed and species concentrations in each case, the mixing residuum r was computed at three positions: at 25%, 50% and 100% of the relative mixer length. In relation with the reciprocal element number an estimation of the numerical errors is possible.

Comparing the numerical simulation results obtained on the 100% mesh with extrapolated values for arbitrary fine meshes we find that typical discretisation errors are below approximately 8%. This indicates that it is not efficient to use calculations with bigger meshes than the 100% mesh to evaluate the different micromixers. It should be mentioned that the results represented in the following do not raise the claim to resolve very detailed flow effects such as microvortexes or similar. This is, on the one hand, not essentially needed to globally assess the devices. On the other hand, expending effort to resolve such detailed effects is contrary to the idea of the approach - obtaining a rough classification of the investigated mixers prior to detailed experimental investigations. The time to achieve convergence for the simulations varied between 2 h and 8 h, depending on investigated micromixer and flow conditions.

5.2. Flow conditions

5.2.1. Y-mixer As expected, the variation of the initiator mass flow ratio influences the flow conditions in the contacting zone. Increasing the ratio of initiator to monomer flow rate leads to a (partial) blocking of the initiator inlet. This gives rise to circulations of the initiator fluid in the contacting zone. Increasing the ratio enhances the extent of circulation (compare Figure 3A and B). As a second effect it was observed that at high initiator/monomer ratios the initiator fluid jackets the monomer fluid. This can lead to a situation where the initiator fluid changes the channel side and flows at the opposite side (Figure 3B). Both effects increase the contact area between the fluids and hence should speed up the mixing process.

5.2.2. Chicane mixer Not surprisingly, a similar situation for the inlet zone was found as for the Y-mixer. Depending on the ratio of mass flow rates, circulations and jacketing of the monomer fluid can be observed. The chicanes indeed deflect the flow, but the introduced transversal forces are relatively weak. Because of this, the chicanes create only slight convection. With regard to the operation conditions chosen the channel dimensions seem to be too large to benefit from flow redirection.

A closer inspection of the flow field reveals that the chicane geometry is not optimal. Dead zones were found which do not contribute to faster mixing and have a negative influence on the residence time distribution (Figure 4A). The flow velocity in these zones is very low and due to that accumulation of reactants and polymers can be expected. Under these conditions, uncontrolled reactions can occur probably leading to fouling problems. Similar flow conditions were previously described in the literature for zigzag channels [59]. The flow

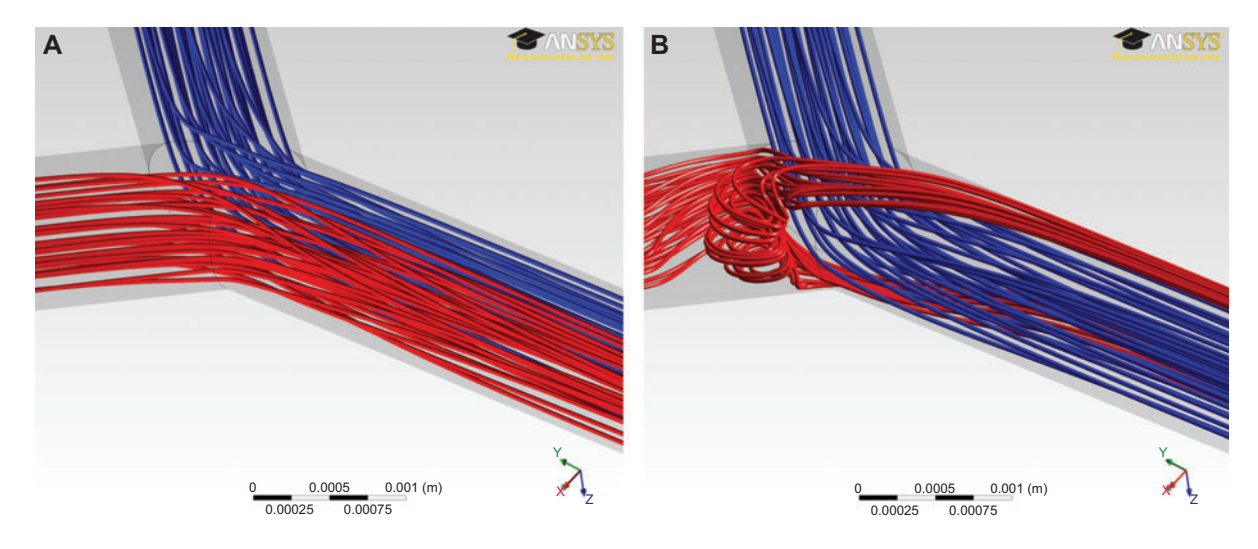


Figure 3 Flow conditions within the Y-mixer for \dot{m}_{Init} =0.03 g/s and \dot{m}_{Init} =0.000283 g/s. Red streamlines show trajectories based on the velocity field of the initiator solution, whereas streamlines coloured in blue represent the monomer solution.

conditions are reflected by the concentration field, indicating a low contribution of convection to the mixing process (Figure 4B).

5.2.3. ST-mixer By contrast, the flow conditions within the ST-mixer are chaotic. The obstacles continuously redirect the fluid. By means of this effect, secondary fluid motion is induced leading to an increase of the contact area. Furthermore, the channel diameter is decreased by the obstacles which, on the one hand, reduces the necessary diffusion length and, on the other hand, increases the flow velocity. Both effects lead to an acceleration of the mixing speed. As described before, the obstacles are intended to realise the split-and-recombine principle. Analysing the flow conditions shows that the SAR principle superimposes the already stated flow patterns but is not the sole mixing principle. It is suppressed by fluid motion leading to unstable lamellar interfaces which prevent the successful formation of the needed flow characteristics.

Figure 5A shows the flow conditions for symmetrical mass flow rates of \dot{m} =0.03 g/s. To better visualise the extent of convection, the concentration field is shown in Figure 5B.

5.2.4. Caterpillar mixer Also within the caterpillar mixer, the SAR principle is not perfectly realised. Under the investigated process conditions transversal forces occur which continuously redirect the fluid within the mixer. Due to internal friction, the fluid lamellae are disturbed and a perfect straight boundary layer cannot be preserved. The transversal forces are strong enough to dominate the flow patterns. The secondary fluid motion observed can be regarded as Dean vortexes (Figure 6). Therefore, the flow conditions can better be described as chaotic advection. The originally intended SAR principle is suppressed. This outcome coincides with published results in the literature [49, 50].

Owing to the fact that the inlets of this mixer are parallel to each other the impact of different fluid ratios is not as high as

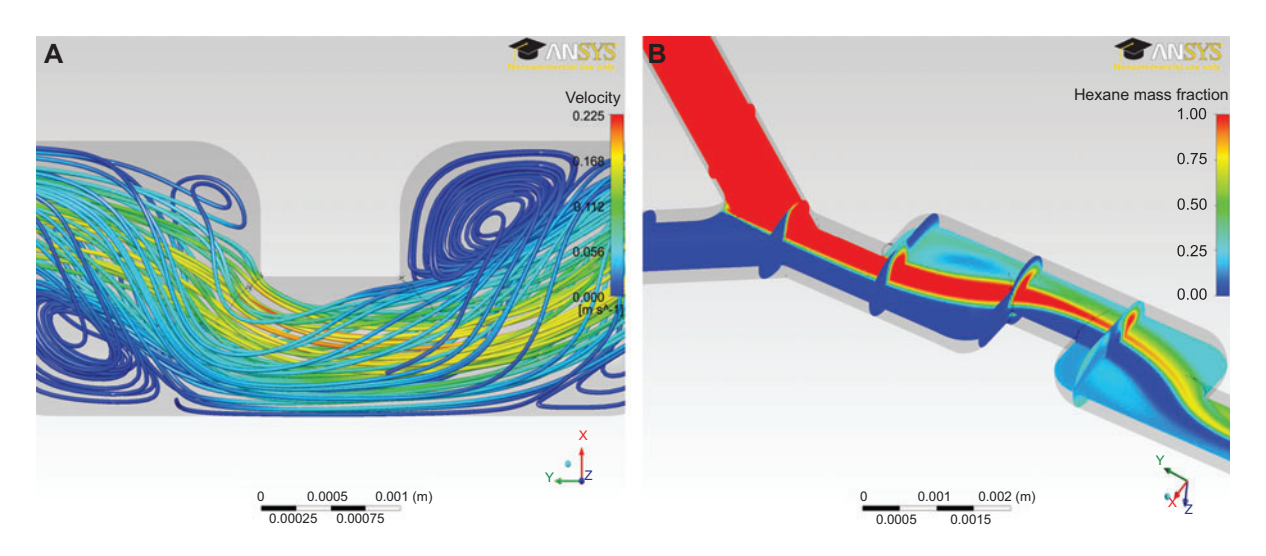


Figure 4 Flow conditions and concentration profile within the chicane mixer for $m_{toi} = 0.03$ g/s.

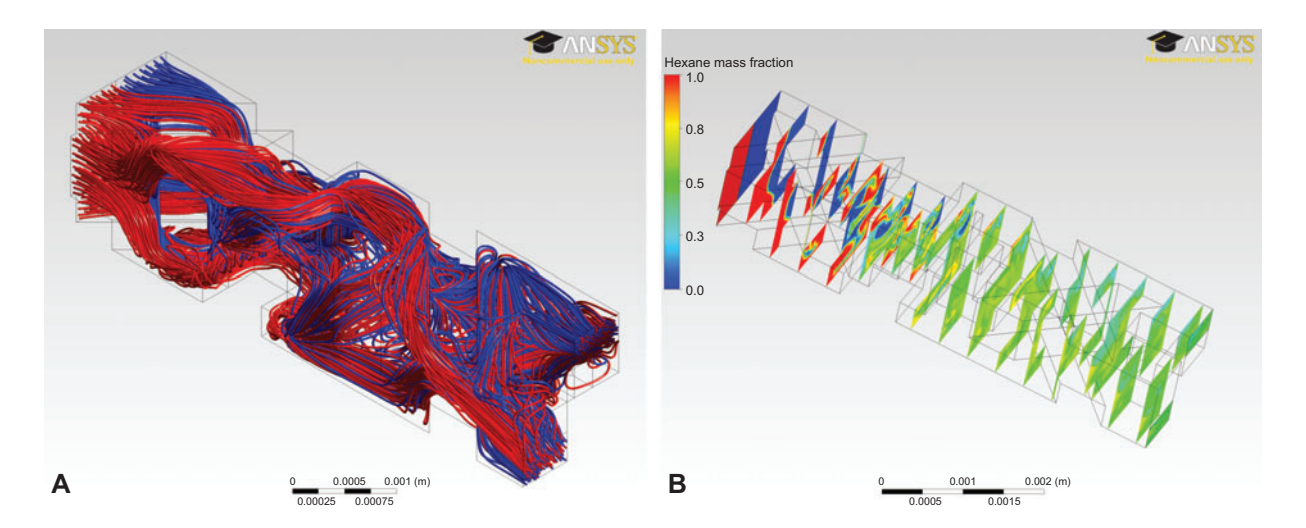


Figure 5 Flow conditions and concentration profile within the ST-mixer for $\dot{m}_{\text{Init}} = 0.03 \text{ g/s}$.

within the Y-mixer or the chicane mixer. Additional vortexes at the inlet were not observed.

The only distinction, resulting from the size differences of the various channel widths, is the flow velocity within the mixers. When using the same flow rates, increasing the channel width from 300 µm to 1200 µm significantly reduces the influence of transversal forces, leading to a lower degree of convection. As a consequence, the overall mixing process is slowed down. For the 1200 µm version the secondary fluid motions are in conflict with the SAR principle. Both effects work against each other. Thus, the contact area between both fluids stays virtually the same. The flow pattern approaches the flow pattern of a bilamination mixer (see Figure 7). As a consequence, convection only slightly contributes to the mixing process.

5.2.5. Interdigital mixer As a consequence of the geometric flow focussing, the flow velocity is drastically increased (Figure 8) [52, 53]. The high velocities together with the very thin lamellae, which are generated within the geometric focussing of the interdigital mixer, lead to problems with numerical diffusion.

Owing to the expected problems of numerical diffusion the simulation results are expected to overestimate the mixing quality to a certain extent. Nevertheless, the mixer was not excluded from the discussion as, on the one hand, experimental data for this mixer was available from inhouse experiments and the literature and, on the other hand, this procedure ensures data consistency. As it was just intended to rank the different micromixers instead of a full quantification of the mixing process, it seems permissible to also classify this type of mixer. It should be pointed out that even experimental methods such as the Villermaux-Dushman test reaction only allow to deliver the order of magnitude of the mixing time [40].

5.3. Mixing performance

5.3.1. General remarks In the following section, the mixing performance of the various mixers is discussed. This is

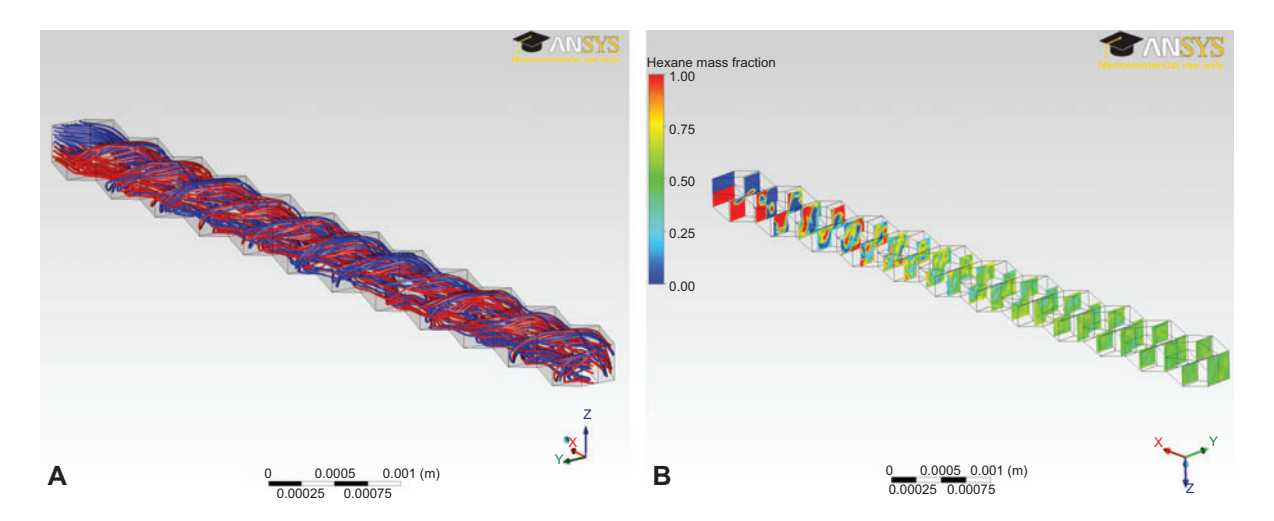


Figure 6 Flow conditions and concentration profile within the 300 μ m caterpillar mixer for $\dot{m}_{\rm ini} = 0.03$ g/s.

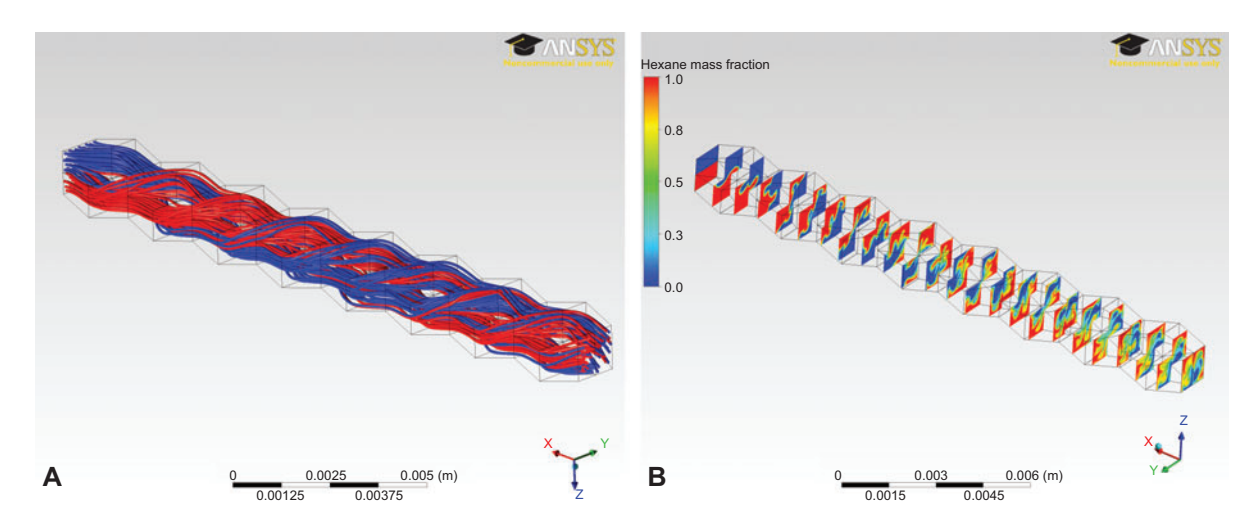


Figure 7 Flow conditions and concentration profile within the 1200 μ m caterpillar mixer for $\dot{m}_{\text{Init}} = 0.03 \text{ g/s}$.

done by using the above-mentioned mixing residuum and the corresponding mixing times, see Eq. (6). The time needed to achieve a 95% mixing quality was used for the assessment.

5.3.2. Comparison of the different mixers by CFD In Figure 9 the time to achieve a mixing quality of 95% for each mixer is plotted against the ratio of mass flow rates. For all mixers where the quality target was not reached within the mixer the time was interpolated. This was possible because for all mixers the mixing residuum showed a linear trend in the last parts of the device. For a better comparison, the space time $t_{\rm R}$ of the mixer was calculated for all mixers. The results are summarised in Table 3.

It was found that the interdigital mixer and the 300 μm caterpillar mixer outperform all other devices by approximately one order of magnitude in mixing time. This can mainly be attributed to the small channel dimensions compared to the other mixers. With this the diffusion lengths are drastically reduced and the mixing process is speeded up. Due to the

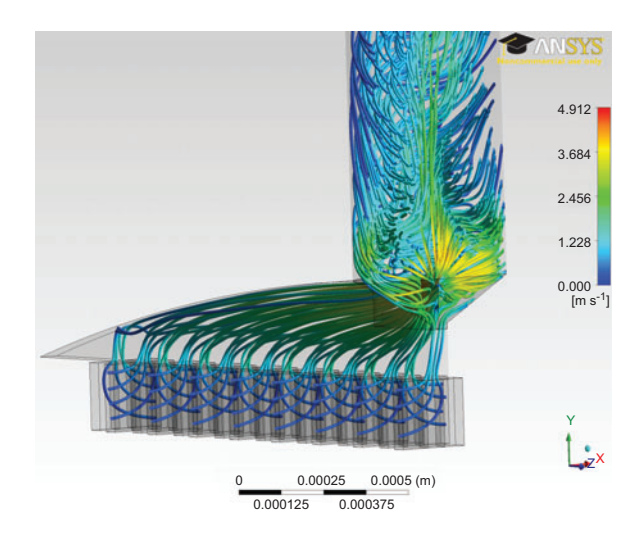


Figure 8 Flow conditions and concentration profile within the interdigital mixer for $\dot{m}_{\rm ini}$ =0.03 g/s.

before-mentioned numerical problems with the interdigital mixer, a clear distinction of the mixer with the shortest mixing time cannot be done. Despite that it can be stated that these two mixers show similar mixing times in the range of 1–30 ms, depending on the ratio between initiator and monomer mass flow rate.

For the caterpillar mixers with larger channel size an increase in the mixing times was found. The mixing time of the 600 μm version ranges from approximately 80 to 250 ms, whereas it lies between 850 ms and 2700 ms for the 1200 μm version.

As the ST-mixer exhibits relatively large channel dimensions, it was not to be expected that the calculated mixing times are in a range of 100–350 ms. However, this result can be attributed to two effects. At first, the internal obstacles permanently redirect the fluid and generate vortexes which enhance mixing. Secondly, the obstacles partially reduce the channel width. Because of this, the lamellar thickness is reduced and the flow velocity is increased, leading to enhanced convection and decreased diffusion length resulting in a speed-up of the mixing process.

The mixing speed decreases slightly while increasing the ratio of monomer to initiator mass flow rates. This probably results from the reduced energy input. The before-mentioned circulations in the inlet zone do not contribute to faster mixing efficiently. The pronounced decrease of the mixing time of the interdigital mixer at very high ratios of initiator to monomer mass flow rates is mainly attributed to numerical problems.

The chicane mixer and the Y-mixer show a similar performance as the 1200 μm caterpillar mixer. Obviously, this is due to the large channel dimensions. The lamellar thickness is too large to ensure sufficient mass transport by diffusion. This especially holds true for the Y-mixer where the only convection results from vortex generating effects at the inlet. Despite the induced convection in the chicane mixer, the mixing performance is low (compare with Figure 4B). Even for this device the degree of fluid motion perpendicular to the flow direction is not adequate for fast mixing. This correlates with the larger channel width, as this is the reason for a lower

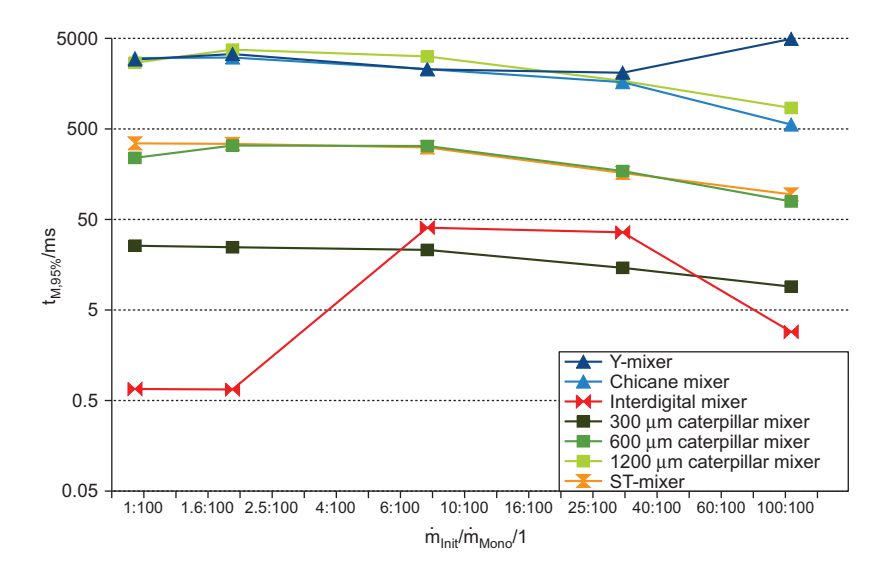


Figure 9 Mixing times to achieve 95% mixing quality as a function of the ratio of initiator mass flow rate to monomer mass flow rate for all investigated micromixers.

fluid velocity and thus reduced transversal forces. The same also applies for the 1200 µm caterpillar mixer. The discussion of the flow patterns within the 1200 µm caterpillar mixer showed that secondary fluid motion and the SAR principle of this mixer work against each other. Mixing can be nearly exclusively attributed to diffusion.

5.3.3. Comparison with results from the literature The CFD results were validated by comparison with the results of Falk et al. based on the results of the villermaux-Dushman test reaction [40]. For this purpose, the mixing time was divided by the square of the characteristic dimension of the mixer and plotted against the Reynolds number. The results are shown in Figure 10. It can be seen that our data fit seamlessly with the literature values.

As mentioned before, the results from Falk et al. represent the mixing performance for symmetrical flows. In our work both symmetric and asymmetric flow conditions were investigated. In the strict sense, only the results for symmetric flow conditions should fit the literature results. Interestingly, our results blend in well with the recently published results, even for asymmetric flow rates.

The Villermaux-Dushman test reaction is only capable of determining the magnitude of the mixing time. With this in mind, the comparison of our CFD data with the experimental data suggests that the resolution of our CFD results is high enough to evaluate different micromixers.

5.3.4. Experimental polymerisation results As previously reported, the presented investigations were done to support experimental work by advising the best suited micromixer for the anionic polymerisation of styrene. Consequently, the acquired results of best suited types of micromixers for our specific task were implemented into experimental work. As the experimentally used process conditions were also applied for the CFD calculations, the performance order gathered by computations should match the experimental order.

Details on the experimental work will be given in a corresponding publication, as the description of the resulting synthesis protocols for rod-coil-copolymers is behind the scope of this article.

A vital part of ongoing research activities was to ensure a narrow molecular weight distribution of the resulting

Table 3 Space times, Reynolds numbers and mixing times for all investigated micromixers and highest and lowest initiator flow rate.

$\dot{m}_{\rm Init}/({\rm g/s})$	0.03			2.83×10 ⁻⁴		
	t _R /ms	Re/1	t _{M,95%}	t _R /ms	Re/1	$t_{ m M,95\%}$
Y-mixer $(d_{h}=1000 \mu \text{m})$	766	174	4940	1799	88	2919
Chicane mixer $(d_h = 1000 \mu \text{m})$	1285	174	559	3016	88	3030
ST-mixer $(d_h=292 \mu \text{m})$	195	469	95	458	237	346
Interdigital mixer $(d_h=106 \mu \text{m})$	13	1293	3	31	652	1
300 μm caterpillar mixer (d_b =300 μm)	8	456	9	20	230	26
600 μm caterpillar mixer (d_b =600 μm)	67	228	79	157	115	239
1200 μm caterpillar mixer (d_h =1200 μm)	357	114	852	838	58	2695

The monomer mass flow rate is constantly \dot{m}_{Inii} =0.03 g/s. Reynolds numbers were calculated at the narrowest cross-section utilising the hydraulic diameter $d_{\rm h}$.

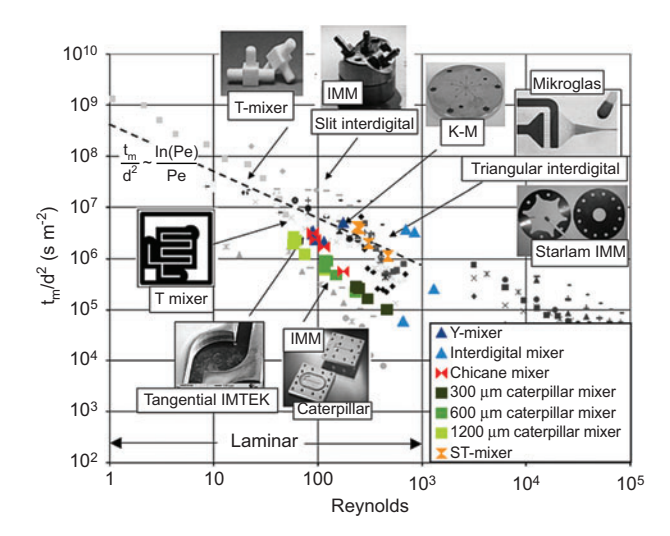


Figure 10 Mixing times normalised by the square of the characteristic flow dimension as a function of the Reynolds number. The results from this work (coloured symbols) were integrated into the results from Falk et al. (Reprinted with permission from Elsevier) [40].

semiconducting polymers with a PDI below 1.2. Following the argumentation that the molecular weight distribution depends on the mixing velocity, this substance property was used as an indicator to judge the mixing performance.

The experimental results (Figure 11 and Table 4) show that the chicane mixer provides a high PDI of 1.8 resulting from a very poor mixing performance whereby the chain growth started uneven. The PDI is even higher than the PDI obtained from batch experiments. This is in accordance with the numerical calculations. Interestingly, the PDIs achieved for the ST-mixer, the interdigital mixer and the 300 μm caterpillar

mixer are identical. For these three mixers a very narrow PDI of 1.07 was achieved.

Based on this we concluded that a narrow molar mass distribution can be achieved under chosen process conditions when the mixing time is reduced down to a calculated threshold value of approximately 200–400 ms. Further acceleration of mixing has no influence on the molar mass distribution. In addition to the mixing process another process seems to limit the overall reaction rate. The limiting process was not clearly identifiable yet, but there are some reasonable explanations.

One possible reason for the retardation of the process could be the behaviour of butyllithium in solution. N-Butyllithium tends to form hexamer clusters in apolar solvents such as n-hexane or cyclohexane. As polymerisation is induced by the monomeric organolithium compound, the butyllithium cluster has to dissociate before the actual reaction starts. With regard to resulting reaction control aspects, this can lead to following situation. As long as the butyllithium molecules are clustered, the probability that the initiation step proceeds is very high. This results, on the one hand, from the faster reaction rate of the initiation step and, on the other hand, from the high local density of the butyllithium molecules. After all clustered molecules had reacted with one styrene molecule, there is a high probability that all chains grow with an equal speed, resulting in a narrow molar mass distribution. This situation remains until the cluster breaks up and every reaction chain diffuses in the solution independently.

It is further known that apolar solvents slow down the reaction rate of anionic polymerisations [60]. Within the experimental work, the initiator butyllithium was solved in hexane, whereas the monomer styrene was solved in THF. Against this background, it seems reasonable that the reaction is retarded as long as the active reaction chains are not solved in THF.

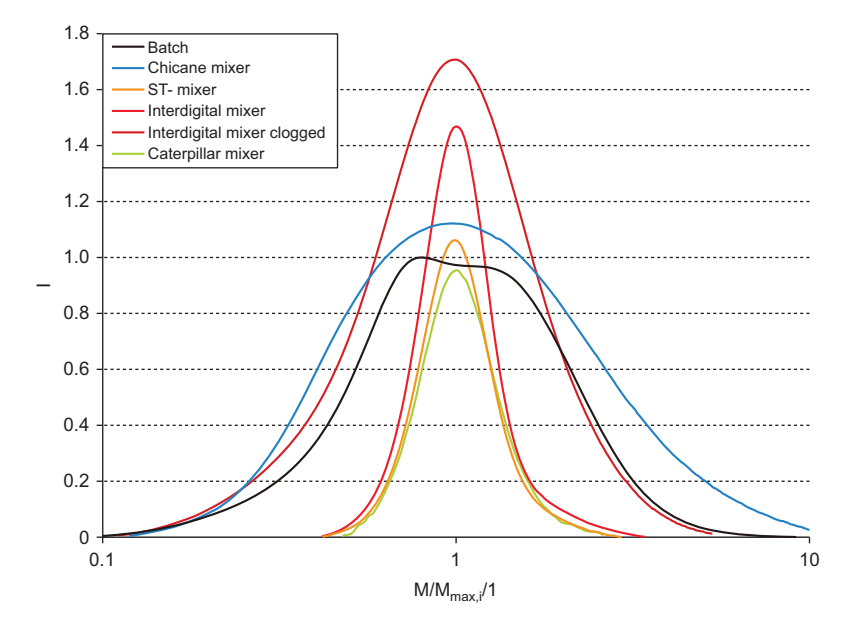


Figure 11 Normalised results from size-exclusion chromatography (SEC) for four investigated micromixers. The molar mass M is normalised to the most frequent molar mass M_{max} . The intensity I of the signal is plotted as measured. A number-average molecular weight of 3000 g/mol was targeted. Achieved values of all samples were between 3000 and 6000 g/mol.

Table 4 PDIs for different micromixers and process conditions.

Mixer	Comment	PDI
Batch	_	1.43
Chicane mixer	_	1.8
ST-mixer	_	1.07
Interdigital mixer	_	1.07
Interdigital mixer	Clogged	1.42
300 µm caterpillar mixer	-	1.07

During the experimental work it was also found that the interdigital mixer suffers from serious clogging problems due to the formation of inorganic residues. Experiments showed that clogging can cause very bad mixing performance with PDIs higher than in batch experiments (Figure 11 and Table 4). In practice, this qualifies the 300 µm caterpillar mixer as the best suited device among the investigated micromixers. However, it should be mentioned that this is not a general result. The results only hold true for the investigated process including the specific process conditions.

6. Conclusion

One vital part for conducting anionic polymerisation reactions, to prepare high quality polymers with narrow PDI, is mixing. To ensure a sufficient reaction control, including fast mixing and heat removal, microstructured devices were chosen for a specific synthesis task. With this choice the question raised which microstructured device is appropriate for the intended polymerisation process. To decrease the experimental effort and the resulting costs, a numerical approach was chosen as a decision support tool during experimental planning. Semi-quantitative CFD calculations were used to determine the best suited micromixer out of a collection of different devices.

For this purpose, different types of micromixers were evaluated. First, a simple Y-mixer and a chicane mixer were factored into the calculations. Further, an interdigital mixer and different split-and-recombine mixers, namely a caterpillar mixer in different versions and a ST-mixer, were included in the assessment.

The mixing process was quantified by a so-called mixing residuum. To compare the different mixers, a mixing quality of 95% was defined as the target and the time needed to achieve this target was used for comparison. The results show that the interdigital micromixer and the 300 µm caterpillar mixer offer the best mixing performance. The ST-mixer and the 600 µm caterpillar mixer show a similar mixing speed, whereas the Y-mixer, the chicane mixer and the 1200 µm caterpillar mixer were found to be not suited for our purposes.

Using a collection of the numerical examined micromixers for experimental investigations, the general order gained from CFD calculations could be confirmed, although it has been found that other effects also had an influence on the resulting polymer properties. Additionally, it was found that a calculated mixing time of approximately 200-400 ms is sufficient. Faster mixing has no experimental advantage.

With this it could be shown that CFD calculations can beneficially be used to rank micromixing devices for specific process conditions. This enables the scientist to reduce experimental effort and the costs involved with it.

Acknowledgements

We want to thank the IMM for providing the Interdigital micromixer and we gratefully acknowledge the financial support from the Deutsche Bundesstiftung Umwelt.

References

- [1] Kompter C, Ziegenbalg D, Kralisch D, Sell S, Klemm E. In 19th International Congress of Chemical and Process Engineering 2010.
- [2] Szwarc M. Nature 1956, 178, 1168-1169.
- [3] Bywater S, Worsfold DJ. J. Polym. Sci. 1962, 58, 571-579.
- [4] Hostalka VH, Figini RV, Schulz GV. Makromol. Chem. 1964, 71, 198-203.
- [5] Hadjichristidis N, Iatrou H, Pispas S, Pitsikalis M. J. Polym. Sci. A Polym. Chem. 2000, 38, 3211-3234.
- [6] Ehrfeld W, Hessel V, Löwe H. Microreactors: New Technology for Modern Chemistry. 1st ed., Wiley-VCH Verlag GmbH & Co. KGaA: Weinheim, 2000.
- [7] Bayer T, Himmler K. Chem. Ing. Tech. 2004, 76, 560-566.
- [8] Hessel V, Löwe H, Schönfeld F. Chem. Eng. Sci. 2005, 60, 2479-2501.
- [9] Hessel V, Hardt S, Löwe H, Müller A, Kolb G. Chemical Micro Process Engineering, 1st ed., Wiley-VCH Verlag GmbH & Co. KGaA: Weinheim, 2005.
- [10] Wirth T, Ed. Microreactors in Organic Synthesis and Catalysis, 1st ed., Wiley-VCH Verlag GmbH & Co. KGaA: Weinheim, 2008.
- [11] Hessel V, Renken A, Schouten JC, Yoshida J, Eds. Micro Process Engineering: A Comprehensive Handbook, Wiley-VCH Verlag GmbH & Co. KGaA: Weinheim, 2009.
- [12] Hessel V, Ehrfeld W, Golbig K, Haverkamp V, Löwe H, Storz M, Wille C. IMRET 3 Proceedings, Springer-Verlag: Berlin,
- [13] Jähnisch K, Baerns M, Hessel V, Ehrfeld W, Haverkamp V, Löwe H, Wille Ch, Guber A. J. Fluorine Chem. 2000, 105,
- [14] Ehrich H, Linke D, Morgenschweis K, Baerns M, Jähnisch K. Chimia 2002, 56, 647-653.
- [15] Löb P, Löwe H, Hessel V. J. Fluorine Chem. 2004, 125,
- [16] Chambers RD, Fox MA, Holling D, Takashi Okazoe TN, Sandford G. Lab Chip 2005, 5, 191-198.
- [17] Steinfeldt N, Abdallah R, Dingerdissen U, Jähnisch K. Org. Process Res. Dev. 2007, 11, 1025-1031.
- [18] Hessel V, Angeli P, Gavriilidis A, Löwe H. Ind. Eng. Chem. Res. 2005, 44, 9750-9769.
- [19] Bally F, Serra CA, Brochon C, Anton N, Vandamme T, Hadziioannou G. Macromol. React. Eng. 2011, 5, 542-547.
- [20] Bally F, Serra CA, Hessel V, Hadziioannou G. Chem. Eng. Sci. 2011, 66, 1449-1462.
- [21] Bayer T, Pysall D, Wachsen O. IMRET 3 Proceedings, Springer-Verlag: Berlin, 2000.

- [22] Wu T, Mei Y, Cabral JT, Xu C, Beers KL. J. Am. Chem. Soc. 2004, 126, 9880–9881.
- [23] Wu MH, Cai HY, Xu X, Urban JPG, Cui ZF, Cui Z. Biomed. Microdev. 2005, 7, 323–329.
- [24] Nagaki A, Kawamura K, Suga S, Ando T, Sawamoto M, Yoshida J. J. Am. Chem. Soc. 2004, 126, 14702–14703.
- [25] Iwasaki T, Nagaki A, Yoshida J. Chem. Commun. 2007, 1263–1265.
- [26] Iwasaki T, Yoshida J. Macromol. Rapid Commun. 2007, 28, 1219–1224.
- [27] Iwasaki T, Yoshida J. Macromolecules 2005, 38, 1159-1163.
- [28] Iwasaki T, Yoshida J. Patent US2006235170, Idemitsu Kosan Co. Ltd., Tokyo, 2006.
- [29] Serra C, Sary N, Schlatter G, Hadziioannou G, Hessel V. *Lab Chip*, 2005, 5, 966–973.
- [30] Schlatter CG, Sary N, Schönfeld F, Hadziioannou G. Microfluid. Nanofluid. 2007, 3, 451–461.
- [31] Mandal M, Serra C, Hoarau Y, Nigam K. Microfluid. Nanofluid. 2011, 10, 415–423.
- [32] Rosenfeld C, Serra C, Brochon C, Hessel V, Hadziioannou G. Chem. Eng. J. 2008, 135, S242–S246.
- [33] Rosenfeld C, Serra C, Brochon C, Hadziioannou G. Lab Chip 2008, 8, 1682–1687.
- [34] Honda T, Miyazaki M, Nakamura H, Maeda H. *Lab Chip* 2005, 5, 812–818.
- [35] Miyazaki M, Honda T, Nakamura H, Maeda H. Chem. Eng. Technol. 2007, 30, 300–304.
- [36] Nagaki A, Tomida Y, Yoshida J. Macromolecules 2008, 41, 6322–6330.
- [37] Nagaki A, Tomida Y, Miyazaki A, Yoshida J. Macromolecules 2009, 42, 4384–4387.
- [38] Wurm F, Wilms D, Klos J, Löwe H, Frey H. Macromol. Chem. Phys. 2008, 209, 1106–1114.
- [39] Iida K, Chastek TQ, Beers KL, Cavicchi KA, Chun J, Fasolka MJ. Lab Chip 2009, 9, 339–345.
- [40] Falk L, Commenge J-M. Chem. Eng. Sci. 2010, 65, 405–411.
- [41] Commenge J-M, Falk L. Chem. Eng. Process. 2011, 50, 979–990.
- [42] Hardt S, Ehrfeld W, Hessel V, Vanden Bussche KM. Chem. Eng. Commun. 2003, 190, 540–559.

- [43] Engler M, Kockmann N, Kiefer T, Woias P. Chem. Eng. J. 2004, 101, 315–322.
- [44] Hoffmann M, Schlüter M, Räbiger N. Chem. Eng. Sci. 2006, 61, 2968–2976.
- [45] Hoffmann M, Schlüter M, Räbiger N. Chem. Ing. Tech. 2007, 79, 1067–1075.
- [46] Dreher S, Kockmann N, Woias P. Heat Transfer Eng. 2009, 30, 91–100.
- [47] Kashid M, Renken A, Kiwi-Minsker L. Chem. Eng. J. 2011, 167, 436–443.
- [48] Schwesinger N, Frank T, Wurmus H. J. Micromech. Microeng. 1996, 6, 99–102.
- [49] Schönfeld F, Hessel V, Hofmann C. Lab Chip 2004, 4, 65-69
- [50] Schönfeld F, Hardt S, Hessel V, Hofmann C. Chem. Ing. Tech. 2004, 76, 614–618.
- [51] Hardt S, Pennemann H, Schönfeld F. Microfluid. Nanofluid. 2006, 2, 237–248.
- [52] Hessel V, Hardt S, Löwe H, Schönfeld F. AIChE J. 2003, 49, 566–577.
- [53] Hardt S, Schönfeld F. AIChE J. 2003, 49, 578-584.
- [54] Aminabhavi TM, Patil VB, Aralaguppi MI, Phayde HTS. J. Chem. Eng. Data 1996, 41, 521–525.
- [55] Ali A, Nabi F, Itoo FA, Tasneem S. J. Mol. Liq. 2008, 143, 141–146.
- [56] Giner B, Gascon I, Villares A, Cea P, Lafuente C. J. Chem. Eng. Data 2006, 51, 1321–1325.
- [57] Bird RB, Stewart WE, Lightfoot EN. *Transport Phenomena*, 2nd ed. Wiley: New York, 2001.
- [58] Huebschmann S, Kralisch D, Hessel V, Krtschil U, Kompter C. Chem. Eng. Technol. 2009, 32, 1757–1765.
- [59] Mengeaud V, Josserand J, Girault HH. Anal. Chem. 2002, 74, 4279–4286.
- [60] van Beylen M, Bhattacharyya DN, Smid J, Szwarc M. J. Phys. Chem. 1966, 70, 157–161.

Received January 24, 2012; accepted March 5, 2012



Dirk Ziegenbalg studied chemistry at the Friedrich-Schiller-University Jena and received his diploma degree under supervision of Prof. G. Kreisel and Dr. D. Kralisch. During this period, he dealt with the "Characterization of microstructured mixers by use of computational fluid dynamics in view of reaction engineering aspects". Currently, Dirk Ziegenbalg is a PhD student and works on the usage of light sources

with low power consumption for photochemical reactions. In combination with microstructured reactors advantages for the overall plant size and the overall energy efficiency are expected.



Christoph Kompter studied environmental chemistry at the Friedrich-Schiller-University Jena and received his diploma degree under supervision of Dr. D. Kralisch in the workgroup of Prof. G. Kreisel. In his diploma project he investigated the implementation of anionic polymerizations in microstructured mixers, receiving polymers with narrow molecular weight distribution. Currently, he is working on his PhD thesis dealing

with different polymerization techniques in micromixers. The emphasis is on emulsion polymerisation with monodisperse distribution and on anionic polymerisation to investigate new ways concerning the synthesis of organic semiconductors.



Friedhelm Schönfeld was born in 1970, he was appointedProfessorforEngineering Mathematics at Hochschule RheinMain - University of Applied Sciences, in 2008. Prior to this, he was Head of the Simulation Group at Institut für Mikrotechnik Mainz GmbH (IMM), Germany. He obtained his PhD in theoretical physics in 1999 at the University of Cologne, Germany.

His research interests focus on computational fluid dynamics, multidisciplinary modelling and environmental sciences. He is author of more than 60 publications and eight patents.



Dana Kralisch studied environmental chemistry at the Friedrich-Schiller-University (FSU) Jena in Germany. Afterwards she worked for 2 years at the Agency for Agriculture of the Federal State of Thuringia. In 2002, she decided to return to the FSU to study the coupling of environmental impact analyses tools and chemical process design. In 2006, she obtained

her PhD degree under the supervision of Prof. Dr. Guenter Kreisel. Since 2007, she has led the "Green Process Design and Evaluation" research group at the Institute of Technical and Environmental Chemistry. Her current research activities focus on topics such as decision support during design, the application of enabling technologies for chemical syntheses and on the biopolymer bacterial nanocellulose.